Effect of Aerosols on Hazardous Species Dispersion

Anil Kumar[1*], and *Amita* Tripathi[2]

[1]FLUIDYN India, Bangalore, India
[2]FLUIDYN France, 93200 Saint-Denis, France

Abstract. Airborne hazardous species such as radioactive nuclides and viruses normally get transported through air by bulk convection and turbulent and laminar dispersion. In addition, their concentration is affected by the deposition onto different surfaces such as walls and floors. This paper studies the effect of aerosols, such as dust particles, on the dispersion of such species in air. Specifically, the attachment of nanometer sized hazardous materials onto the micron sized aerosols and the subsequent transport of the former by the latter is modelled and investigated using numerical methods. It involves a 3D, transient CFD based model to simulate the transport of the aerosols of different sizes. It is found that with normal aerosol particle concentration the dispersion pattern and hence the decay rate of the smaller sized particles mostly follows that of the larger sized aerosols.

1 Introduction

Many airborne hazardous substances or pollutants are particulate in nature. Progenies of radioactive materials such as radon and thoron are examples for this [1] [2]. Radon is a natural source of radiation coming from the bedrocks and therefore present in confined spaces, such as workplaces and housings. It has been shown to be a cause for cancer. Therefore, the mechanisms of dispersion of radon particles, especially in polluted environments such as urban environment need to be understood. Typically, the particulate clusters are of sizes ranging from a few nanometers to tens of nanometers and at least an order of magnitude smaller than the typical aerosols. The transport of these pollutants involves convection, diffusion, decay and formation, just like a gaseous species. However, in addition to these, they may get attached to or detached from the larger sized aerosols. Hence, their transport could be highly influenced by the behaviour of the aerosol transport itself. The transport of such materials is characterized by two parts: (1) fine fraction and (2) coarse fraction. The part which is not attached to the aerosol is called fine fraction and the part attached to the aerosols is called the coarse fraction. Figure 1 illustrates these two with respect to radio-nuclide progenies.

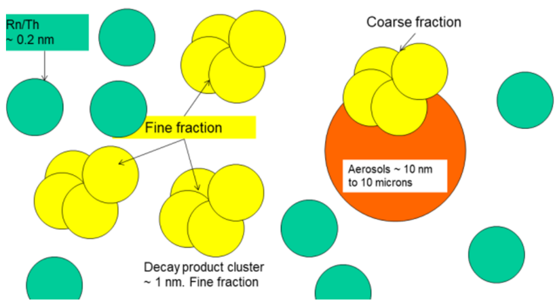

Fig. 1: Fine fraction and coarse fraction of particulate matter.

This paper presents a CFD based 3D model to simulate the fine and coarse fractions of a pollutant. It involves models for air flow, convection, dispersion and deposition of aerosols and fine fractions. The air flow is modelled using 3D, unsteady Navier-Stokes equations for turbulent flow. The aerosols and fine fractions are modelled using scalar transport equations. In addition, a model to calculate the rate of attachment of the fine fractions to the aerosols, thus forming the coarse fractions, is introduced.

The following sections present the equations and solution methodology and the simulation results for the transport of aerosols and fine and coarse fractions for a set of radio-nuclide progenies in a ventilated room.

2 Equations and solution method

The equations and methods used for air flow modelling and their testing and validation are given in [3] along with the equations for the transport of aerosols, fine and coarse fractions in [4]. This section gives the governing equations for the transport of gaseous species, which

* Corresponding author: anil.kumar@fluidyn.com

will not get attached to aerosols, fine fractions and coarse fractions. The first ones, i.e., pollutants remaining as gaseous species, are modelled using the following convective-diffusive scalar transport equation:

$$\frac{\partial(\rho Y_0)}{\partial t} + \nabla \cdot \left(\rho \vec{V} Y_0\right) = \nabla \cdot (\rho D_0 \nabla Y_0) + S_{Y,0} - \lambda_0 \rho Y_0 \quad (1)$$

The diffusion coefficient, D_0, is the sum of the molecular and turbulent diffusion coefficients. The transport equation for the fine fraction of the j^{th} pollutant in a chain of products is of the form:

$$\frac{\partial\left(\rho Y_j^f\right)}{\partial t} + \nabla \cdot \left(\rho \vec{V} Y_j^f\right) = \nabla \cdot \left(\rho D_j^f \nabla Y_j^f\right) - \left(\lambda_j + \lambda_{j,a} + \lambda_{wj}^f\right)\rho Y_j^f + \lambda_{j-1}\rho Y_{j-1}^f + r\delta_{j,2}\lambda_{j-1}\rho Y_{j-1}^c \quad (2)$$

These equations are written assuming that the (j-1)th pollutant can decay into j^{th} pollutant and the j^{th} pollutant can decay into (j+1)th pollutant and so on. The equation for the coarse faction takes the form:

$$\frac{\partial\left(\rho Y_j^c Y_a\right)}{\partial t} + \nabla \cdot \left(\rho \vec{V} Y_j^c Y_a\right) = \nabla \cdot \left(\rho D_a \nabla Y_j^c\right) - \lambda_j Y_j^c Y_a + \lambda_{j,a}\rho Y_j^f + \left(1 - r_j\right)\lambda_{j-1}^f \rho Y_{j-1}^c + \lambda_{j-1}\rho Y_{j-1}^f Y_a + S_{g,j}^c \quad (3)$$

The effective diffusivity for fine fraction, D_j^f, is calculated using the models for Brownian motion and turbulent diffusion. The effective attachment coefficient, λ_a, in a poly-dispersed aerosol environment depends on the aerosol size distribution through the equation [5]:

$$\lambda_{j,a} = \int_0^{\infty} \beta(D_j^f, D_a) N_a(D_a) dD_a \quad (4)$$

where $\beta(D_j^f, D_a)$ is the attachment coefficient for the aerosol diameter D_a and $N_a(D_a)$ is the size distribution function of the number density. For a finite number of particle sizes λ_a is calculated numerically as

$$\lambda_{j,a} = \sum_{i=1}^{i=n} \left(\beta(D_j^f, D_{a,i}) \times N_{a,i}\right) \quad (5)$$

where n is the number of particle sizes (sections) used and $N_{a,i}$ is the number density of the i^{th} particle size. The attachment coefficient, $\beta(D_j^f, D_{a,i})$, for the i^{th} particle size is calculated as follows:

$$\beta(D_j^f, D_{a,i}) = \frac{2\pi D_j^f D_{a,i}}{\frac{8D_j^f}{D_{a,i} v_0} + \frac{D_{a,i}}{D_{a,i} + 2l_0}} \quad (6)$$

where v_0 is the thermal velocity and l_0 is the mean free path length. The mass diffusivity of the fine fraction, D_j^f, is the sum of Brownian and turbulent diffusivities:

$$D_j^f = D_{j,b}^f + D_{j,t}^f \quad (7)$$

Brownian diffusivity is calculated as

$$D_{j,b}^f = \frac{k_b T C_u}{3\pi \mu_l d_{p,j}^f} \quad (8)$$

where, k_b is the Boltzmann constant, T is the temperature, C_u is the Cunningham slip correction factor, μ_l is the laminar viscosity, and $d_{p,j}^f$ is the diameter of the fine fraction.

Cunningham slip correction factor, C_u, is calculated as a function of the molecular mean free path of the fluid:

$$C_u = 1 + \frac{l_0}{d_{p,j}^f}\left[2.34 + 1.05\, exp\left(-0.39\frac{d_{p,j}^f}{l_0}\right)\right] \quad (9)$$

Molecular mean free path, l_0 is calculated using the viscosity, pressure, temperature and molecular weight of the fluid:

$$l_0 = \frac{\mu_l}{p}\sqrt{\frac{\pi R_u T}{2M_f}} \quad (10)$$

Thermal velocity is calculated using the local and instantaneous fluid temperature, T, and the molecular weight of the fine fraction:

$$v_0 = \sqrt{\frac{8R_u T}{\pi M_{ff}}} \quad (11)$$

The coefficients for wall deposition, λ_{wj}^f and λ_{wj}^c, can be calculated using the local flow field if criteria and physical models for wall absorption are available. Otherwise, it can be a uniform and constant parameter. The diffusion coefficient for the aerosol, D_a, will be calculated using the models for Brownian motion and turbulent diffusion for the aerosols. The term S_g^c is due to the movement of aerosols relative to the local air flow and will be a function of the local aerosol size distribution. The equation for coarse fraction will be formulated such that it conforms to the equation for aerosol distribution.

The scalar transport equations 1-3 along with the Navier-Stokes equations for air flow are solved numerically using an implicit finite volume method.

3 Simulations

3.1 Geometry and Flow Conditions

The simulation domain is a test chamber with an inlet and an outlet (Figure 2). The details are given in [6] and [7]. The test chamber is of the dimensions (2.5 m × 2.5 m × 2.5 m). It has an inlet of size (0.07 m × 0.07 m) and an outlet of the same size. The air flow through the inlet is at a velocity of 0.443 m/s, which is equivalent to an air change rate of 0.5 h^{-1}.

Outlet at 2.2 m from the floor, 1.25 m from the side

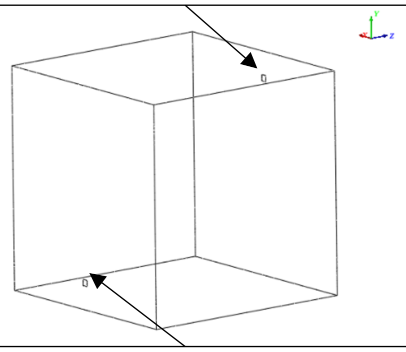

Inlet at 0.3 m from the floor, 1.25 m from the side

Fig. 2: Geometry of the test chamber

3.2 Aerosol Simulations

First, the simulations of the airflow and aerosol transport corresponding to those reported in Figure 7 of [7] are performed and the results are compared. In this case, once the air flow field has become steady, the whole domain is initialised with a uniform concentration of aerosols of different sizes. The aerosol diameters used in the current simulations are 0.35, 1.31, 1.8, 3.5, 6.25 and 12.5 microns, respectively. One of the results calculated is the decay rate. It is defined as the ratio of the rate of decrease of aerosol concentration to the instantaneous aerosol concentration. It can be calculated locally or on a volume average basis. The aerosol concentration can decrease, or decay, either due to deposition on to the surfaces or due to outflow or both. Figure 3 shows the comparison of the average deposition decay rates obtained with those reported by [7] and the current results match well.

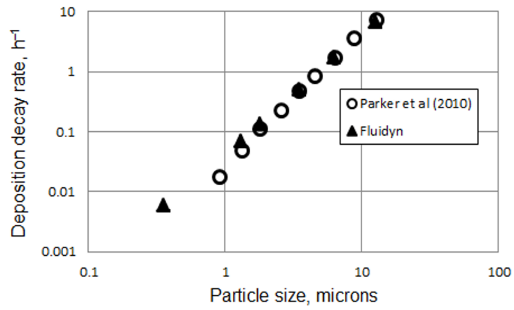

Fig. 3: CFD average deposition decay rate comparison

3.3 Fine and Coarse Fraction Simulations

These simulations consider the transport of ^{220}Rn and its progenies in the presence of aerosols. Among the progenies only ^{216}Po, ^{212}Pb and ^{212}Bi are considered, because of the shorter simulation duration considered compared to the relevant half life periods. The results demonstrate the effect of attachment of pollutants to the aerosols. For these simulations, the domain is initialized with zero velocity field and a constant velocity of 0.443 m/s is specified at the inlet. Also, the whole domain is intialized with a monodispersed aerosol of the size 12.5 microns and a number density of 10^{10} m^{-3} and ^{220}Rn with a concentration of 10^5 units/m^3. The radionuclide progeny clusters are assumed to be of the size of 2 nm.

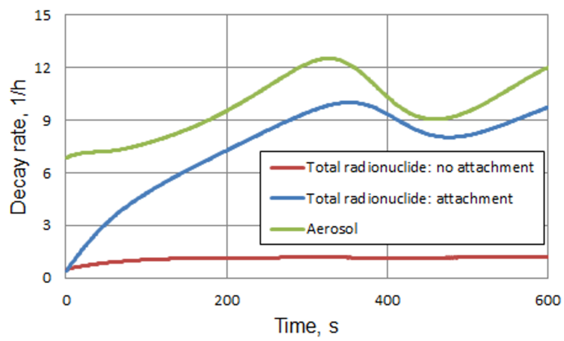

Fig. 4: Total radionuclide and aerosol decay rate.

Figure 4 shows the evolution of the decay rates of the total radio nuclides and the aerosol. When the attachment of the pollutant nanoparticles to the aerosols is not considered, then the decay rate is about 1 h^{-1}. In this case there is only fine fraction. However, when the attachment is considered, i.e., when the fine and coarse fractions are present, then the decay rate is highly influenced by the decay rate of the aerosols. It can be seen that, in the beginning the decay rate of the total radionuclides is less than that of the aerosols, or it is lagging it qualitatively. This is because of the delay due to the finite attachment rate.

4 Conclusions

A numerical model for the simulation of transport of fine and coarse fractions of nanometer sized particulate

materials is developed. The attachment of fine fractions to the background aerosols is modelled. It is found that for the typical values of aerosol concentrations the transport of these particulate materials, both the ventilation and the deposition onto the walls, is greatly influenced by the aerosol transport. The total decay rate of the total quantity almost follows that of the aerosols for the scenario considered.
These conclusions help in understanding the interaction of indoor pollutants such as natural radioactive particles or airborne viruses with urban air quality.

5 References

1. UNSCEAR *Sources and Effects of Ionizing Radiation*: Report to the General Assembly with Scientific Annexes United Nations, New York. (2000)
2. World Health Organization, *WHO handbook on indoor radon: a public health persepective*, (2009)
3. Agarwal, T. K., Sahoo, B. K., Kumar, M. and Sapra, B. K., *A Computational Fluid Dynamics Code for Aerosol and Decay-Product Studies in Indoor Environments*, Journal of Radioanalytical and Nuclear Chemistry, (2021)
4. Agarwal, T. K., Sahoo, B. K., Joshi, M., Mishra, R., Meisenberg, O., Tschiersch, J. and Sapra, B. K., *CFD Simulations to Study the effect of Ventilation rate on 220Rn Concentration Distribution in a Test House*, Radiation Physics and Chemistry, 162, pp. 82-89 (2019)
5. Biermann, A. H. and Sawyer, S. S. *Attachment of Radon Progeny to Cigarette-Smoke Aerosols*, UCRL-CR-120647, Lawrence Livermore National Laboratory (2015)
6. Bouilly, J., Limam, K., Beghein, C., and Allard, F. *Effect of ventilation strategies on particle decay rates indoors: An experimental and modelling study*. Atmospheric Environment, 39, 4885–4892 (2005)
7. Parker, S., Nally, J., Foat, T. and Preston, S. *Refinement and testing of the drift-flux model for indoor dispersion and deposition modelling,* Journal of Aerosol Science, 41, pp. 921-934. (2010)